

ORIGINAL RESEARCH PAPER

Analyzing the effect of quinalphos pesticide on fish health through molecular docking studies and their eradication by photocatalytic degradation using Fe/S/TiO₂ nanocomposite

Anisha Russelraj^{1*}, Sibmah Stalin¹, Kirupa Vasam Jino¹

¹ Department of Chemistry & Research Centre, Nesamony Memorial Christian College (Affiliated to Manonmaniam Sundaranar University, Abishekapatti, Tirunelveli-627 012), Marthandam, Tamilnadu, India

Received: 2023-08-18

Accepted: 2023-11-18

Published: 2024-01-31

ABSTRACT

Because of growing environmental issues, there is a requirement for the immediate degradation of pesticides and their residues from local and commercial streamlets. Quinalphos is one of the most common organophosphorous pesticides especially used in agricultural fields brings about a great impact on the environment, thereby affecting the health of aquatic organisms and humans. Among the various types of methods that have been implemented, photocatalytic reaction is considered the most relevant technique for the removal of toxic organic contaminants. In this study, modified TiO₂ has been synthesized by doping with Fe, S (Fe/S/TiO₂) using a simple one-step sol-gel method. Different spectroscopic methods, including X-ray diffraction (XRD), SEM with EDAX, diffuse reflectance spectroscopy (DRS), transmission electron microscopy (TEM), and Fourier-transform infrared spectroscopy (FT-IR), were used to assess the structural, morphological, and optical characters of the synthesized catalyst. The incorporation of Fe³⁺ and the distribution of S nonmetal in the TiO₂ crystal lattice were affirmed by the XRD, SEM, and FT-IR analysis. The band gap energy of the Fe/S/TiO₂ nanocomposite has been narrowed to 2.5eV and its photocatalytic activity has been extended to the visible region. The photocatalytic performance of Fe/S/TiO₂ was studied through the photodegradation of Quinalphos. The photocatalytic activity of the respective nanocomposites on the degradation of Quinalphos has been confirmed by UV-visible spectroscopy. Thus, Fe/S/TiO₂ photocatalyst was employed for the degradation of Quinalphos and complete mineralization was achieved in 12 minutes of visible light irradiation, and it was analyzed by TOC analysis. The determination of reaction intermediates has also been carried out. The reaction rate followed pseudo - first-order kinetics. Furthermore, the reusable feature of the catalyst was demonstrated to be used for twelve cycles. The penetration of pesticide residues into protein pockets of fishes was predicted by molecular docking. Furthermore, the reduction in toxicity level of the effluent was examined using aquatic organisms. Thus, Fe/S/TiO₂ nanocomposite is an efficient photocatalyst to oxidize emerging organic contaminants due to its high synergetic effect of visible light absorbing tendency and low recombination effect of charge carriers.

Keywords: Modified TiO₂ Photocatalyst, Pesticide Residues, Fish Protein, Visible Light, Mineralisation.

How to cite this article

Russelraj A., Stalin S., Jino K. V., Analyzing the effect of quinalphos pesticide on fish health through molecular docking studies and their eradication by photocatalytic degradation using Fe/S/TiO₂ nanocomposite. J. Water Environ. Nanotechnol., 2024; 9(1): 99-111. DOI: 10.22090/jwent.2024.01.07

INTRODUCTION

Water is a basic requirement for everyone's life. The major worldwide challenge for the twenty-first century is to furnish and ensure safe water for the entire ecosystem. Water pollution can be caused by a variety of factors, including agricultural runoff from pesticides and fertilizers, wastewater

discharged directly into rivers or streams, and other activities [1]. At present, water pollution caused by pesticides is a critical issue. Due leaching, runoff, and drifting of these harmful chemicals in water systems cause toxic effects on aquatic and other living organisms. Several pesticides have been utilized during the past decades to protect crops from pests. The pesticides tremendously increase

* Corresponding Authors Email: anisharusselraj@gmail.com



This work is licensed under the Creative Commons Attribution 4.0 International License.

To view a copy of this license, visit <http://creativecommons.org/licenses/by/4.0/>.

the crop yield; simultaneously, they pose a grave threat to the stability of the ecosystem. Pesticide residues enter the body of terrestrial, aerial, and aquatic organisms through inhalation, skin contact, and food consumption. Some possible changes occur after exposure, such as nausea, breathing problems, damage to reproductive organs, and neurological disorders.

Quinalphos is an organophosphate pesticide applied in Indian cultivation fields for controlling caterpillar and scale insects on fruit, trees, cotton, vegetables, sugarcane, nuts, coffee, and rice [2]. Quinalphos affects the respiratory system and further creates irritation to the skin and eyes. The residues of Quinalphos pesticide get easily dispatched from the soil to underground water streams, rivers, and oceans, thereby contaminating them [3]. The uncontrolled usage of pesticides and industrial chemicals for paper, leather, paint, and wood conservation units has given rise to an acute contamination of water. The excessive usage of Quinalphos pesticide has degraded the environment and threatened the existence of non-target life forms, including fish, and fauna by affecting their cholinergic systems.

When large quantities of pollutants are released, there may be an immediate and direct impact on aquatic organisms. This can be measured by large-scale sudden mortalities of fish resulting from the contamination of water with agricultural pesticides. Alleged pollution-related diseases include epidermal fin or tail rot, gill disease, liver damage, neoplasia, and ulceration. Generally, pesticides deteriorate the health of fish by impairing their metabolic processes, which occasionally cause the death of fish. Fishes are particularly sensitive to the environmental contamination of water [4]. Quinalphos pesticide significantly causes serious impairment to the physiological and health status of fish. Hence, the eradication of Quinalphos pesticide from aquifers is a matter of great concern.

Several advanced techniques, like coagulation, flocculation, reverse osmosis, ion exchange method, and ultrafiltration, have been used to eliminate toxic organic contaminants from wastewater. However, the main drawback of these methodologies is the formation of byproducts that cannot be treated again and dumped as such. The present study aims to furnish a suitable remedial technique for the complete mineralization of the pesticide Quinalphos before it gets discharged directly or indirectly into water bodies. The

photocatalysis is an advanced oxidation process (AOP) that is used for the photodegradation of toxic organic compounds. This process helps to convert the composition of organic pollutants entirely into H_2O , CO_2 , and other nontoxic compounds without conveying other secondary pollution [5, 6].

Only a handful of studies have been attempted to examine the photocatalytic degradation of Quinalphos pesticide present in water matrices. Pandey et al prepared S doped TiO_2 photocatalyst that could degrade Quinalphos in 180 minutes. Lingaraj et al investigated the effect of TiO_2 /RGO nanocomposite for degrading Quinalphos in 90 minutes using a mercury vapor lamp. Nidhi et al studied the solar photocatalytic degradation of Quinalphos and reported 87.5% degradation within 240 minutes using Mn-N-co-doped TiO_2 . Kaur and Sud (2012) have investigated the degradation of Quinalphos and have documented the degradation in 180 minutes using TiO_2 in the presence of UV light irradiation. Garg et al considered the photocatalytic activity of GO-ZnO nanoflowers for the degradation of Quinalphos in 45 minutes under UV irradiation. Apart from this literature, the present work has suggested a commercial degradation method to degrade the Quinalphos effluent present in water using a minimum amount of Fe/S/ TiO_2 nanocomposite (0.25 mg) in just 12 minutes under sunlight.

In the present study, the threats posed by pesticides to fish life, high binding efficiency, and the effect of Quinalphos pesticide with particular targets of protein molecules in fishes have been taken into account. A prominent molecular docking technique can be used to examine the interaction energy between the pesticide and the protein. 4BDT, 2AZ5, 1BMA (PDB ID) interacted with Quinalphos, and its effects were measured by the formation of nervous, intestine, and eye disorders in fishes using the PyRx virtual screening tool. Furthermore, in the current study, Fe/S/ TiO_2 nanocomposite was fabricated by sol-gel method in a different approach for the first time and has been investigated for the degradation of Quinalphos using sunlight as a source of visible light. The reduction in toxicity is also evaluated by growing Adult Guppy fish and their death ratio was also calculated.

Furthermore, in the current study, Fe/S/ TiO_2 nanocomposite was fabricated by the sol-gel method in a different approach for the first time and has been investigated for the degradation of

Quinalphos using sunlight as a source of visible light. The structural, morphological, compositional, band gap energy and fluorescent properties of the prepared nanocomposite were examined, and the mineralization of Quinalphos pesticide was confirmed by TOC and UV-Vis spectral analysis. The intermediates produced during degradation and the plausible mechanism have also been studied.

MATERIALS AND METHODS:

All the chemicals used were of analytical grade. The chemicals were utilized as received without further purification. Titanium (IV) isopropoxide and Ethanol were purchased from Iso-Chem laboratories in Kochi (India) respectively. Nitric acid, Iron (III) nitrate, and Thiourea were purchased from Merk Specialties Pvt. Ltd. Mumbai (India). Doubly distilled water was used throughout the experiment.

Preparation of undoped TiO₂:

10 mL of Titanium (IV) isopropoxide was dissolved in 10 mL of ethanol (C₂H₅OH) with constant stirring for about 10 minutes using a magnetic stirrer. To this above suspension, 10 mL of double distilled water was added dropwise to bring about hydrolysis. This solution was further stirred for two hrs till it was transformed into a gel. The gel was allowed to stand for 24 hrs aging and further, it was calcinated to 400 °C to get the undoped TiO₂.

Preparation of Fe/S/TiO₂ nanocomposite:

To synthesize Fe/S/TiO₂ nanocomposite, a sol-gel route was employed. A desired amount of undoped TiO₂ was added dropwise to a minimum quantity of ethanol (C₂H₅OH) with constant stirring. The precipitation of the corresponding hydroxide was prevented by the addition of nitric acid (HNO₃). To the above suspension iron (III) nitrate [(Fe (NO₃)₃·9H₂O)] was added and heated to 50°C. The reaction mixture was magnetically stirred for 3 hours with the addition of thiourea (CH₄N₂S). Finally, 5 ml of double distilled water was added to induce gelation. The gel was dried at 80° C for 3 hrs before being calcined in a muffle furnace at 450° C for 2 hrs.

Characterization

The crystalline size and crystalline phase of the synthesized photocatalyst were calculated by

powder XRD Bruker D8 Advance diffractometer using Ni-filtered Cu K α radiation ($\lambda=1.5406 \text{ \AA}$) as an incident light in 2 θ mode over a range of 20-80° operated at 40 kV, and 30 mA. The presence of functional groups and the nature of the photocatalyst were identified using FT-IR (AVATAR 370) using a Jasco FTIR-4600. The optical properties were evaluated using DRS analysis (Agilent Cary 5000) with BaSO₄ as the reference material. The surface morphology along with its elemental composition was calculated by SEM (FEI Quanta FEG 200F) equipped with an Energy Dispersive X-ray (EDS) Spectrophotometer operated at 30kV and HR-TEM, (JEOL-2100) with a rising voltage of 200 kV and resolution point 0.194nm.

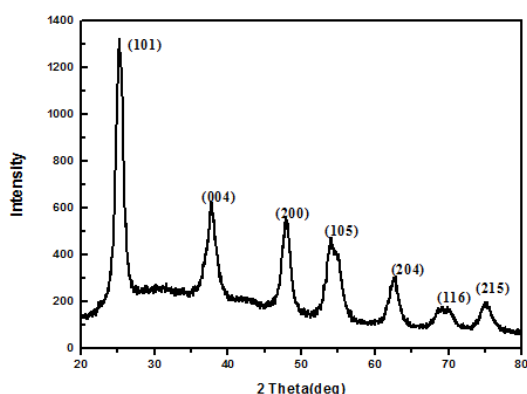
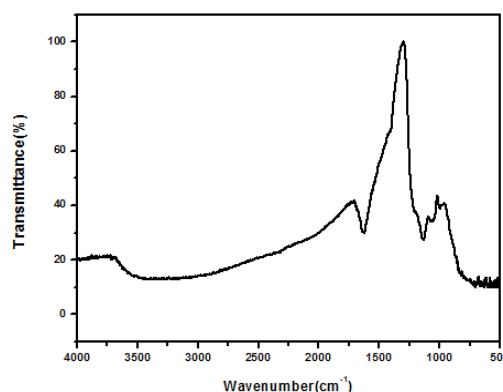
RESULTS AND DISCUSSION:

X-ray diffraction Studies

Fig. 1 depicts the XRD pattern of the Fe/S/TiO₂ nanocomposite. The diffraction peaks at 2 θ values of 25.4°, 48°, 54.7°, and 63.1° are due to the reflections from (1 0 1), (2 0 0), (1 0 5), (2 0 4), (2 2 0) and (2 15) planes. These diffraction peaks correspond with standard JCPDS Card No. 21-1272 and are in close agreement with the anatase phase of the TiO₂ structure. The characteristic peaks at 2 θ values of 30.15°, 35.42°, 43.11°, 53.51°, 56.99°, 62.64°, 74.67° can be indexed to (220), (311), (400), (422), (511), (440) and (533) planes of cubic crystal system of iron nanoparticles, respectively [7]. The ionic radius of Fe³⁺ (0.64Å) is closer to that of Ti⁴⁺ (0.68Å), and it can therefore be easily integrated into the TiO₂ lattice [8]. The presence of monoclinic sulfur has shown a sharp and strong diffraction peak at 2 θ = 28° correlated to the monoclinic structure of sulfur (JCPDS card no: 24-0735). Based on Scherrer's formula, the average crystallite size of the Fe/S/TiO₂ nanocomposite was calculated to be 6.5 nm respectively.

FT-IR Analysis

The vibration bands of the Fe/S/TiO₂ nanocomposite were determined by the FT-IR analysis, ranging from 500 to 4000 cm⁻¹ as displayed in Fig. 2. In Fe/S/TiO₂ nanocomposite, the broad, intense band is located at 1130 cm⁻¹ due to the stretching vibration of Ti-O-Ti linkages in TiO₂ nanoparticles which proves the formation of TiO₂ [9]. Moreover, the absorption band within the region of 900–1300 cm⁻¹ in Fe/S/TiO₂ nanocomposite is a characteristic peak for the formation of the Ti-O-S network. The peak at 1609

Fig. 1. XRD pattern of Fe-S doped TiO₂Fig. 2. FT-IR spectra of Fe-S doped TiO₂

is assigned due to the surface hydroxylation upon doping TiO₂ with Fe. A small peak at 645 cm⁻¹ is a characteristic peak for sulfur [10]. The bands at 3218 cm⁻¹ and 1621 cm⁻¹ correspond to O-H bending and stretching vibrations of absorbed water molecules respectively, which shows the presence of OH ions in the sample. This may positively contribute to the photocatalytic activity of the synthesized nanocomposite.

Morphological and elemental analysis

The morphology of the prepared sample was studied using SEM and TEM analysis. The SEM micrograph of the synthesized Fe/S/TiO₂ photocatalyst is shown in Fig. 3 a. The surface morphology analysis demonstrates the irregular and crystalline form of the nanoparticles. The ultrafine nanoparticles are distributed randomly, and the brighter portions have ensured the doping of iron and sulfur on the surface of TiO₂. The synthesized nanocomposite was aggregated due to the magnetic properties of ferrite nanoparticles [11]. The photocatalytic activity of the catalyst was enhanced by the rough surface of the catalyst.

From the HR-TEM image depicted in Fig. 3 b the lattice fringes with an interplanar distance of 0.20nm are in coincidence with the (101) plane of anatase TiO₂. This confirms that the synthesized nanoparticles are in crystalline form [12]. Fig. 3 e shows the SAED pattern of Fe/S/TiO₂ photocatalyst with concentric rings relating to the standard diffraction plane of anatase. The particle size of Fe-S codoped TiO₂ was analyzed from TEM images using Image J software. The Fe/S/TiO₂ photocatalyst was discovered to have an average particle size of 6.5 nm, which is closely in line with the XRD pattern. Moreover, their size distribution

is presented in the form of a histogram in Fig. 3 f.

The elemental analysis of the Fe/S/TiO₂ nanocomposite was performed by the EDX technique to confirm the existence of the desired elements, as displayed in Fig. 3 g. The EDX spectrum shows four separate peaks for titanium (Ti), iron (Fe), sulfur (S), and oxygen (O), which signifies the incorporation of Fe and S within the TiO₂ matrix. In other words, the obtained product is not a mixture of Fe, S, and TiO₂ nanoparticles but is a nanocomposite. Furthermore, the synthesized catalyst was presumed to be free from metallic impurities, as no other peaks were detected in the spectra. The weight percentage of titanium, iron, sulfur, and oxygen is 49.24%, 4.24%, 3.83%, and 42.69% respectively.

Optical absorption properties:

The optical properties of Fe/S/TiO₂ nanocomposite were analyzed from their absorption spectra. The UV-Vis DRS spectra are depicted in Fig. 4 a and the Tauc plot is displayed in Fig. 4 b. A small peak at 297 nm Tauc plot was generated from UV-Vis spectra by using the Kubella-Munk function, which is used to measure the band gap energy of the synthesized nanoparticles. Due to the doping of Fe and S in the TiO₂ crystal lattice, the Tauc plot demonstrated a shift in peak absorption edge to a longer wavelength region (ie. Redshift), and also an enhancement in the photodegradation performance towards the visible region. The band gap energies of the pure and Fe-S codoped TiO₂ photocatalysts were found to be 3.2 eV and 2.5 eV respectively. This construction of the band gap of synthesized Fe-S codoped TiO₂ is thought to be the result of the mixing of the p orbital of a sulfur atom with the 2p orbital of TiO₂ and the mixing of

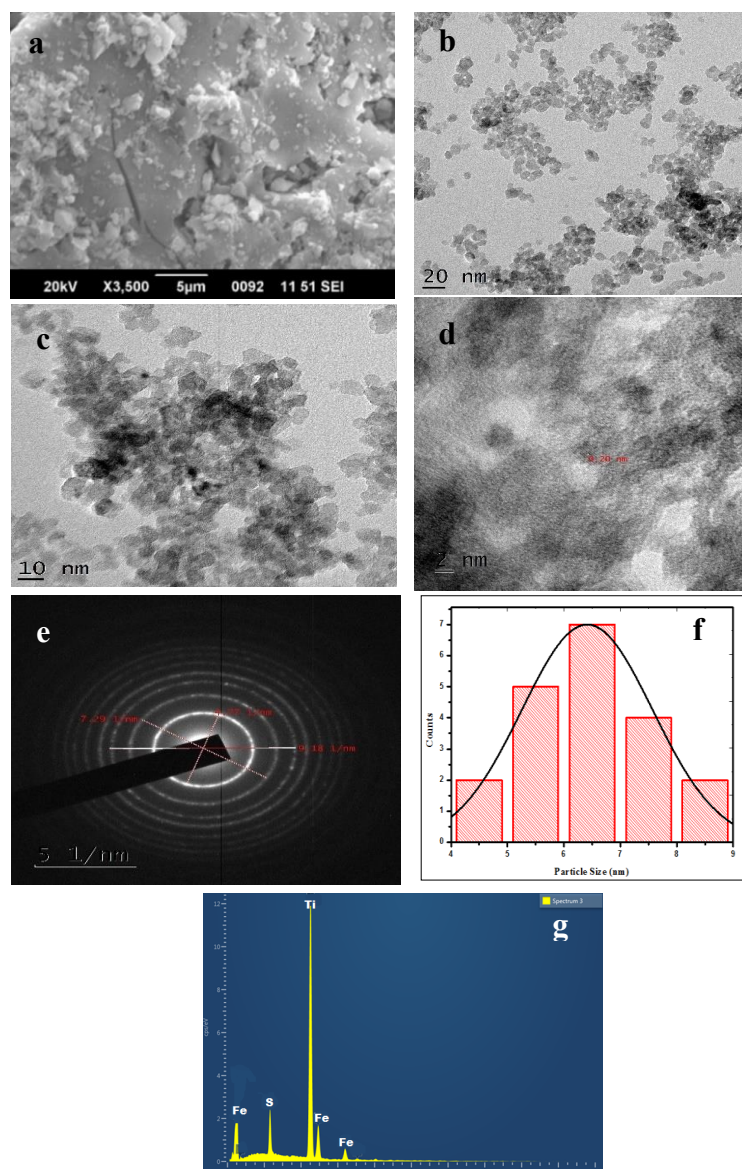


Fig. 3. (a) SEM images of Fe/S/TiO₂, (b, c, and d) HRTEM images of Fe/S/TiO₂, (e) SAED pattern of Fe/S/TiO₂, (f) particle size distribution of Fe/S/TiO₂, (g) EDX image of Fe/S/TiO₂ nanocomposite.

Fe-3d with Ti-3d, which produced localized defect levels slightly above the TiO₂ valence band [13, 14]. These findings suggest that Fe-S codoped TiO₂ could be used as a potential visible-light-driven photocatalyst.

Docking study:

A prominent molecular docking technique can be used to examine the effect of the interaction between the pollutant and proteins. Quinalphos pesticide molecule was docked using the PyRx virtual screening tool. We have docked three proteins 1bma, 2az5, and 4bdt with our target

ligand Quinalphos. We found the following best results with each of the proteins. Among the test candidates in this study, 1bma displayed the highest binding energy of -2.8 kcal/mol and the binding energy of 4bdt -2.6 kcal/mol is lower. The binding affinity is given in Table 1.

Effect of Quinalphos on protein molecules:

The docking study has confirmed the penetration of Quinalphos pesticide into the proteins (1bma, 2az5, and 4bdt). According to the results, hydrogen bonding plays an essential role in the interaction of Quinalphos with proteins, and

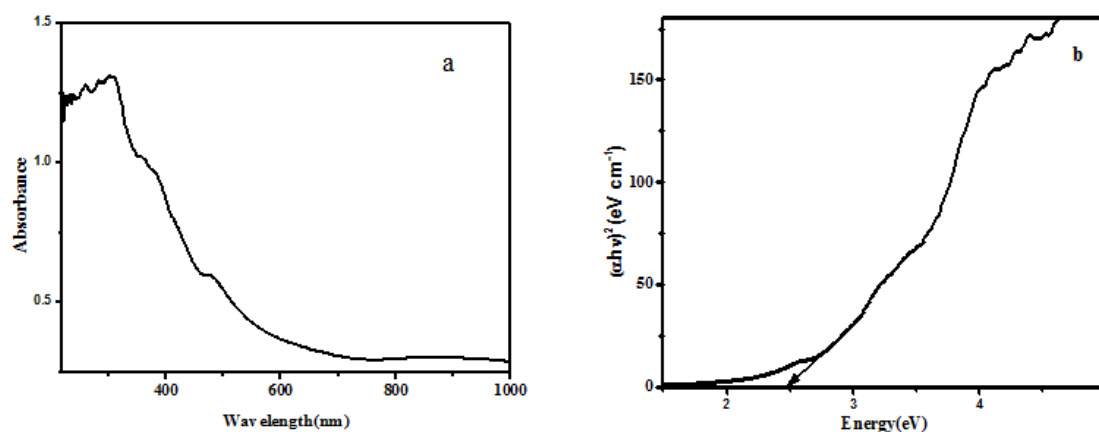


Fig. 4. (a) UV-Vis spectra of Fe-S doped TiO₂ (b) Optical band gap (Eg) spectra of Fe-S doped TiO₂

Table 1. Docking score of Quinalphos pesticide with proteins

Compound	Indices	Protein	Docking score kcal/mol	H- Bonding	H-Bonding distance
Quinalphos	Eye	1bma	-2.8	UNL	1.1
Quinalphos	Intestine	2az5	-2.7	UNL	2.2
Quinalphos	Nerves	4bdt	-2.6	UNL	1.8

finally, the structure of the protein gets denatured [15]. Hence, the protein can no longer perform its function resulting in the loss of activity in the eye, intestine, and nerves. The docked image of the compound is shown in Fig. 5 (a, b, c).

Photocatalytic activity:

The photocatalytic performance of Fe/S/TiO₂ nanocomposite (0.25 mg) was evaluated by degrading Quinalphos pesticide (30 ppm) at neutral pH in the presence of sunlight. Typically, the mixed solution of Fe/S/TiO₂ nanocomposite and Quinalphos was stirred for 30 min in the darkness to achieve the equilibrium of adsorption-desorption before photodegradation [16, 17]. The Photocatalytic experiment was conducted at ambient temperature, and the blended suspension was exposed to sunlight at an intensity of 276 mw/cm². The dispersion (3 mL) was taken every 4 minutes, centrifuged immediately to remove the catalyst, and used for subsequent analysis. The degradation was monitored by UV-visible spectroscopy at 240 nm, the λ_{\max} of Quinalphos. The degradation percentage was calculated using eqn. (1)

$$\text{Efficiency of degradation (\%)} = \frac{C_o - C}{C_o} \times 100 \quad (1)$$

Time-dependent spectra of Quinalphos degradation:

UV-visible absorption spectra were noticed at various intervals for 30 ppm of the pesticide solution to confirm the degradation of Quinalphos using nanocatalysts. The peak of maximum absorption before irradiation was ascertained at a wavelength of 240 nm. The devaluation in absorption in the observed peak concerning the irradiation time of 12 minutes was displayed in Fig. 6. A reduction of reaction time to 12 minutes with a photocatalyst is a significant consequence of the present study.

Degradation mechanism:

The photocatalytic mechanism of the synthesized Fe/S/TiO₂ nanocomposite for degrading Quinalphos pesticide was suggested as follows,

When Fe/S/TiO₂ nanocomposite is irradiated by visible light, it can absorb and give rise to photogenerated electrons (e⁻) and holes (h⁺) which can participate in photocatalytic reactions. The photogenerated holes (h⁺) act as a strong oxidizing agent, and the electrons (e⁻) in the conduction band act as a reducing agent to bring about the degradation of Quinalphos pesticide into small molecules, such as CO₂ and H₂O. The mechanism for radical formation is depicted in Fig. 7.

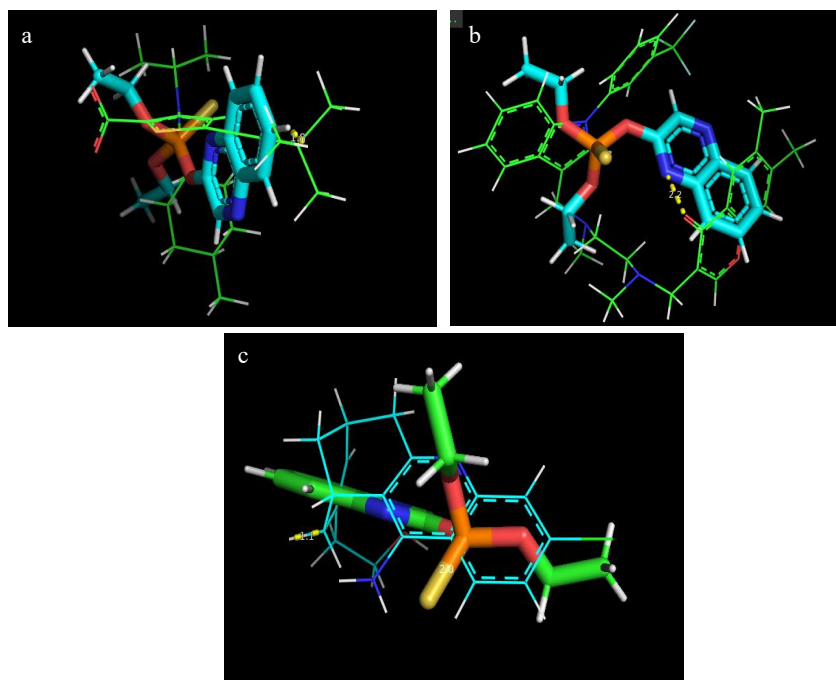


Fig. 5. (a) Docking image of Quinalphos with 1bma (b) Docking image of Quinalphos with 2az5 (c) Docking image of Quinalphos with 4bdt

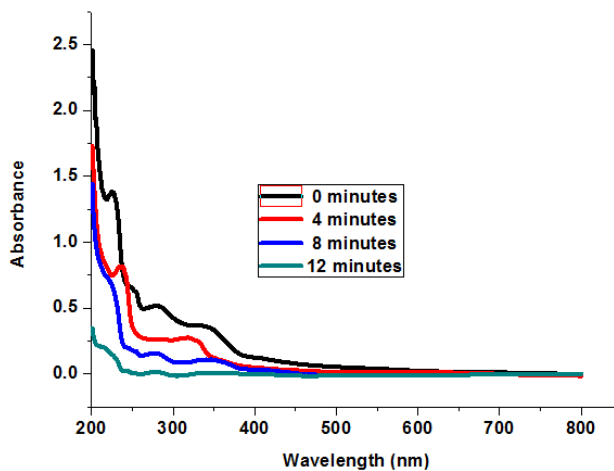
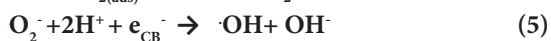
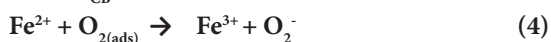


Fig. 6. UV-visible absorption spectrum for degradation at various intervals of time at neutral pH



ESI-MS analysis for Quinalphos pesticide degradation:

To identify the possible intermediates/products and propose plausible photodegradation pathways,

the reactant solutions were analyzed by ESI-MS at the end of the photo-degradation reaction. Fig. 8 shows the mass spectra of Quinalphos after degradation for 20 minutes. The intermediates and products were identified based on the m/z ratio and compared with previous reports. The main mass signals were observed at m/z 298, 130, 170, 169, and 114 in the ESI-MS spectra respectively. The fresh Quinalphos pesticide gives a highly intense single peak at $m/z = 298$ corresponding to the M^+ molecular ion of Quinalphos. Different

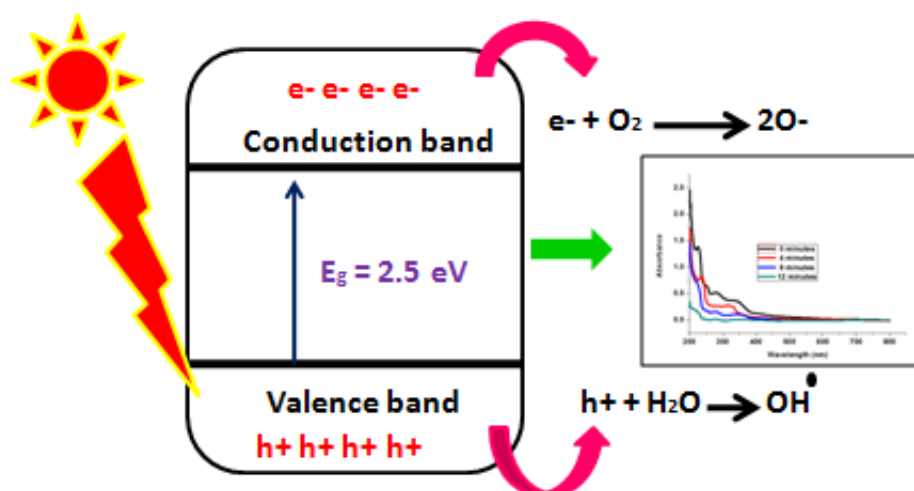


Fig .7. Mechanism for radical formation in photocatalysis.

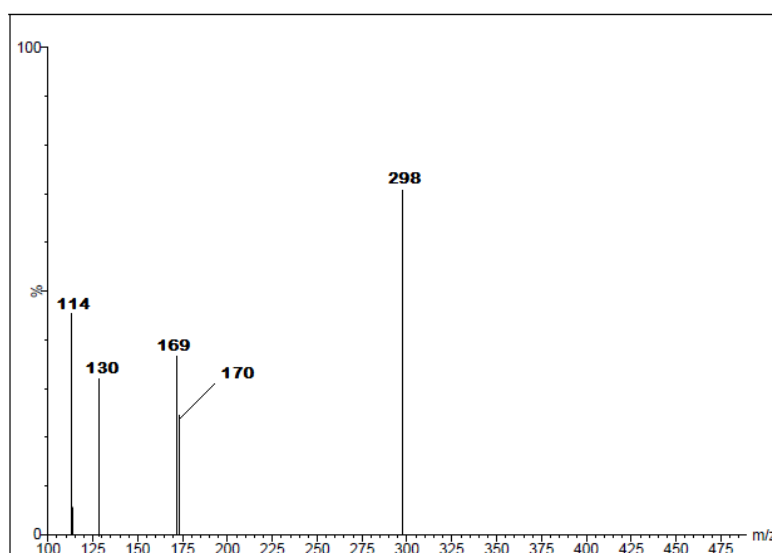


Fig. 8. ESI-MS spectrum for the identification of intermediates for the degradation of Quinalphos

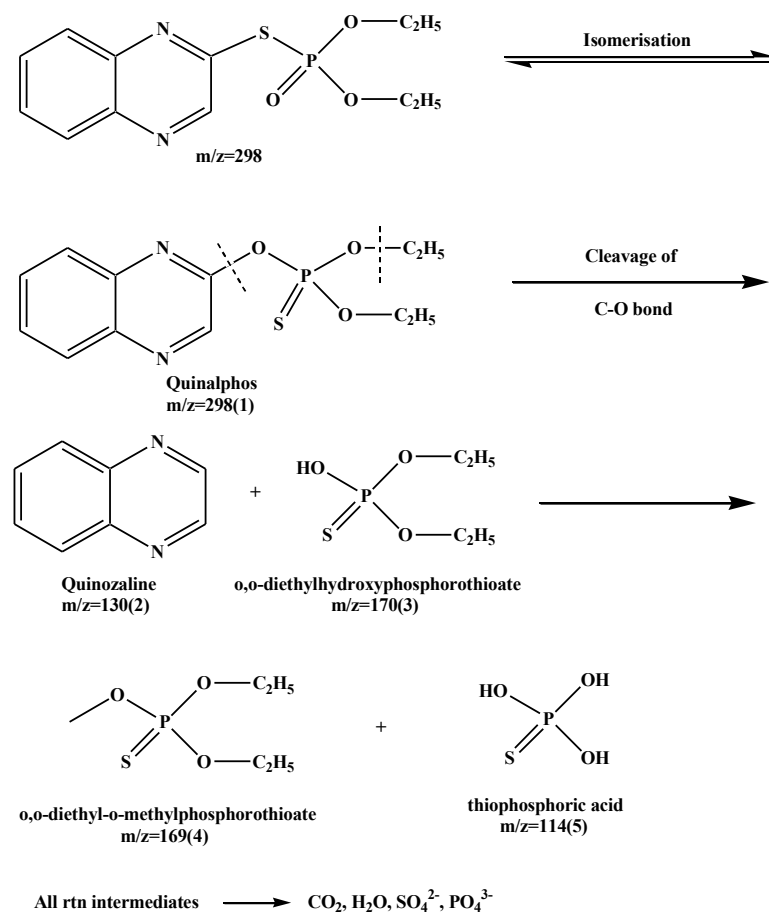
probable intermediates were formed during the photodegradation process of Quinalphos. The analysis of the mass spectrum suggests a sequence of degradation mechanisms as given in the figure. The degradation of Quinalphos (1, m/z 298) is initiated by the attack of hydroxyl radicals at the benzene ring, i.e. C₂ and C₃ carbon of the heterocyclic ring in Quinalphos molecule. The compound (1, m/z 298) undergoes cleavage of the C-O bond to produce an intermediate named, quinoxaline (2, m/z 130) and O, O-diethyl hydroxylphosphorothioate (3, m/z 170).

The compound O, O-diethyl hydroxylphosphorothioate (3, m/z 170)

further oxidizes to produce O, O-diethyl-O-methylphosphorothioate (4, m/z 169) and thiophosphoric acid (5, m/z 114). Finally, this smaller product undergoes mineralization to form CO₂ and H₂O as shown in Scheme 1. This result indicated the ability of ZnO/GO/Cu nanocomposite to mineralize Quinalphos pesticide under visible light irradiation in 12 minutes.

Total organic carbon (TOC) analysis

The removal of carbon content and breakdown of the complex structure of Quinalphos pesticide molecules into smaller and harmless intermediates can be assured by using the TOC analyzer



Scheme 1- Proposed degradation pathway for Quinalphos pesticide

[18]. TOC analysis was executed for 30 ppm of Quinalphos solution at neutral pH in the presence of 0.2 mg/100 mL Fe/S/TiO₂ nanocomposite, for a total period of just 12 minutes. The initial TOC of Quinalphos was 7560 mg/L, which was reduced to 40.28 mg/L after 12 minutes of irradiation under direct sunlight. From these results, the complete mineralization of Quinalphos pesticide by Fe/S/TiO₂ photocatalyst can be finalized.

Comparison with literature data:

To investigate the performance of the synthesized Fe/S/TiO₂ nanocomposite a comparative study has been carried out for various modified TiO₂ photocatalysts available in the literature as displayed in Table 2. From this report, it was observed that the synthesized Fe/S/TiO₂ nanocomposite has exposed a marvelous activity for the degradation of Quinalphos in a short period with a minimum dosage of photocatalyst at neutral pH in the presence of sunlight.

Effect of Quinalphos pesticide on aquatic organisms:

Pesticide contaminants are the major contributors to chemical pollutants that enter aquatic bodies and affect aquatic biota. Adult Zebrafish, obtained from a supplier, were grown in laboratory conditions for 15 days. The fish were kept in glass aquaria at a temperature of 29 °C, fed with ordinary fish food regularly, and exposed to both treated and untreated Quinalphos solutions for about 15 days. Aquarium water was used as a negative control. The relative mortality rate of the fish under analysis was calculated using the formula given below,

$$\text{Relative mortality rate (\%)} = \frac{M_1 - M_2}{M_1} \times 100 \quad (7)$$

Where M_1 and M_2 are the initial and final counts of fish alive respectively.

This data agrees that the mortality rate increases under toxic conditions. However, the rate of mortality decreases in treated water as displayed in Table 3.

Table 2. Comparitive study based on literature dataa

Catalyst	Catalyst Dosage	Concentration of Quinalphos	pH of the test solution	Time (min)	Percentage of degradation	References
Visible/ Bi ₂ O ₃ /TiO ₂	1 g/L	20	8	100	92.0	Sud et al.
Visible/Mn/S/ TiO ₂	1 g/L	25	7	240	98.0	Sharoti et al.
Sunlight/ S/TiO ₂	0.5 g/L	20	6	180	98.1	Sraw et al.
Fe/S/TiO ₂	2 mg/L	30	7	12	100	present study

Table 3. The mortality number from fish in 15 days

Number of days	Untreated water (number of dead fish from 10 fish)	Treated water (number of dead fish from 10 fish)	Aquarium water (number of dead fish from 10 fish)
0	0	0	0
5	2	0	0
10	3	1	0
15	4	0	0
Total	9	1	0
Death ratio	90%	10%	0%

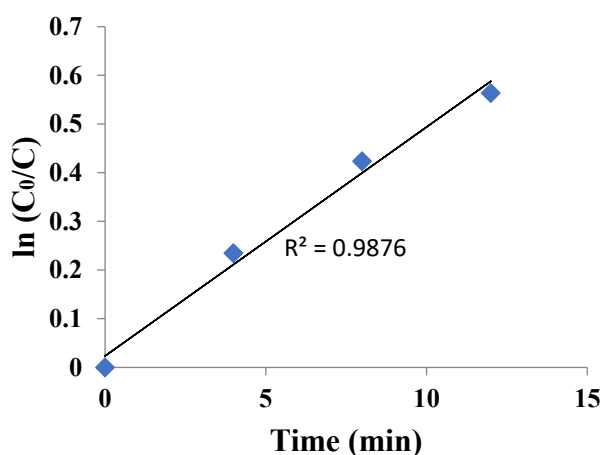


Fig. 9. Kinetics of photocatalytic degradation experiment

Kinetics of the photocatalytic degradation of Quinalphos pesticide:

It has been widely found that the degradation rate of different contaminants via heterogeneous photocatalytic oxidation follows the Langmuir–Hinshelwood (L-H) kinetics model. This model provides the following relationship between the degradation rate and substrate concentration, and the relationship is given as,

$$\ln \frac{C_0}{C} = kt \tag{8}$$

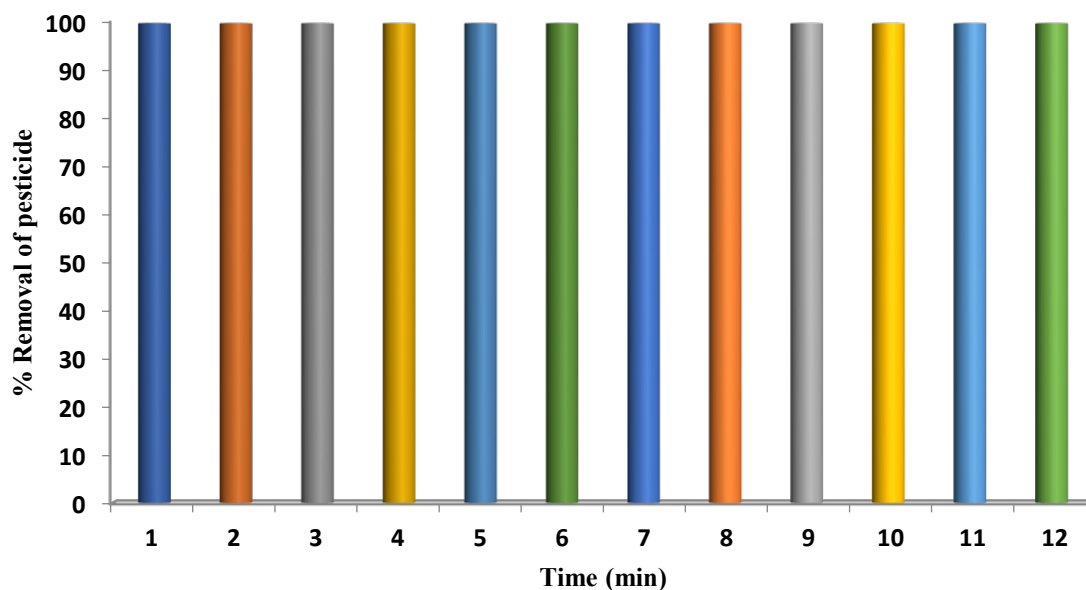
Where C_0 is the initial concentration after irradiation time t , and k is the Pseudo–first–order rate constant [19, 20, 21]. The Langmuir–Hinshelwood

(L-H) kinetics model was used to describe the photocatalytic degradation rate of Quinalphos by plotting the graph of $\ln (C/C_0)$ versus time t , Pseudo–first–order rate constant was determined from the slope of the straight line as displayed in Fig. 9. From the slope, the rate constant k , for the photocatalytic degradation of Quinalphos pesticide using Fe/S/TiO₂ nanocomposite is calculated. The photocatalytic rate constant k for this reaction was determined to be $0.046 \times 10^{-3} \text{ min}^{-1}$ and the regression value is 0.998.

Stability and reusability of Fe/S/TiO₂ nanocomposite:

Apart from the photocatalytic activity, stability and repeatability are also essential for practical



Fig. 10. Recycling ability of Fe/S/TiO₂ photocatalyst

application [22, 23, 24, 25]. Henceforth, the recycling ability of the Fe/S/TiO₂ nanocomposite for the degradation of Quinalphos was examined under consecutive photocatalytic conditions. The photocatalytic experiment was repeated several times to analyze the reusability of the Fe/S/TiO₂ photocatalyst, and the results are seen in Fig. 10. At the end of each cycle, the nanocomposite was washed with double distilled water and then dried in the air. As a result, the Fe/S/TiO₂ nanocomposite has exhibited an incredible photocatalytic performance by enhancing overall stability with twelve reusing cycles. Therefore, the synthesized Fe/S/TiO₂ nanocomposite has shown good stability and turnover frequency when compared with other photocatalysts.

CONCLUSION

In the present study, the diffusion of Quinalphos pesticide within the protein pockets of fishes was authenticated from a molecular docking study. Subsequently, the elimination of Quinalphos pesticide in the water matrix was successfully executed by using Fe/S/TiO₂ photocatalyst in the presence of sunlight. The presence of iron, sulfur, and anatase phases of TiO₂ was confirmed by XRD analysis. The SEM images displayed the doping of iron and sulfur on the surface of TiO₂. The FT-IR analysis has assured the formation of metal oxide nanocomposite. The results have demonstrated that Fe/S doping can greatly increase the visible light

photocatalytic performance of TiO₂ through the introduction of impurity bands in the band gap of TiO₂. The photocatalytic activity of the respective photocatalyst on the degradation of Quinalphos was confirmed by UV-visible spectroscopy. The maximum TOC reduction of 99 % was obtained using Fe/S/TiO₂ photocatalyst (0.25 mg/mL) at neutral pH over a reaction time of 12 minutes without the addition of any oxidizing agents. The kinetic study of the degradation process is observed to follow pseudo-first-order kinetics. Moreover, the Fe/S/TiO₂ catalyst has a good stability and recycling ability of about 12 cycles for the photodegradation of Quinalphos and is found to be cost-effective. The toxicity reduction was successfully estimated by measuring the mortality rate of zebrafish by culturing them in treated water. Hence, this study provides an economy eco-friendly solution to the water treatment problem. Therefore, Fe/S/TiO₂ nanocomposites are promising agents and highly beneficial for various potential applications for the treatment of organic contaminants present in water in a short period.

CONFLICTS OF INTEREST

The authors declare there are no conflicts of interest.

ACKNOWLEDGMENT

The authors are thankful to Nesamony Memorial Christian College, Marthandam,

India, The Sophisticated Analytical Instruments Facility, Chennai, India, Sophisticated Test and Instrumentation Centre, Cochin, India, and the University Science Instrumentation Centre, Alagappa University, Karaikudi, India for furnishing necessary provision and support for this work.

REFERENCES:

- Jayachamarajapura Pranesh Shubha, Kiran Kavalli, Syed Farooq Adil, Mohamed E. Assal, Mohammad Rafe Hatshan, Narsimhaswamy Dubasi, Facile green synthesis of semi conductive ZnO nanoparticles for photocatalytic degradation of dyes from textile industry: A kinetic approach, Journal of King Saud University-Science, 34, (2022), 1-9, DOI: <https://doi.org/10.1016/j.jksus.2022.102047>
- Renuka Garg, Renu Gupta, Nirmal Singh, Ajay Bansal, Eliminating pesticide Quinalphos from surface waters using synthesized Go-ZnO nano flowers: characterisation, degradation pathways and kinetic study, Chemosphere, 286, 2022, 1-12, DOI: <https://doi.org/10.1016/j.chemosphere.2021.131837>
- Paramjeet Kaur, Priti Bansal, Dhiraj Sud, Heterostructured nanophotocatalyst for degradation of organophosphate pesticides from aqueous stream, Journal of the Korean chemical society, 57, (2013), 382-388, DOI: <https://doi.org/10.5012/jkcs.2013.57.3.382>
- Mohammad Malakootian, Alireza Nasiri, Amir Naser Alibeigi, Hakimeh Mahdizadeh, Majid Amiri Gharaghani, Synthesis and stabilisation of ZnO nanoparticles on a glass plate to study the removal efficiency of acid red 18 by hybrid advanced oxidation process, Desalination and water treatment, 170, (2019), 325-336, DOI: <https://doi.org/10.5004/dwt.2019.24728>
- Mehmet Resit Tayssi, Muammer Kirici, Mahinur Kirichi, Burak Tuzun, Alireza Poustforoosh, Antioxidant enzyme activities, molecular docking studies, MM-GBSA, and molecular dynamic of chloropyrifos in freshwater fish Capoeta umbla, Journal of biomolecular structure and dynamics, (2023), 1-14, DOI: <https://doi.org/10.1080/07391102.2023.2192807>
- Deepak Singhwal, Amita Khatri, Pawan Rana, Influence of CTAB surfactant on the various properties of CdO nanoparticles and their application in the field of dye degradation, Journal of water and environmental nanotechnology, 8, (2023), 190-205, DOI: <https://doi.org/10.22090/jwent.2023.08.002>
- Somaiyeh Dadashi, Reza Poursalehi, Hamid Dalavari, Structural and optical properties of pure iron and iron oxide nanoparticles prepared via pulsed Nd: YAG laser ablation in liquid, Procedia materials science, 11, (2015), 722-726, DOI: <https://doi.org/10.1016/j.mspro.2015.11.052>
- Sima Kalantar, Akram Bemani, Mohammad Hossein Sayadi, Elham Chamanehpour, Visible light - driven ZnO/FeO magnetic nanoparticles for detoxification of diazinon: the photocatalytic optimisation process with RSM-BBD model, Environmental science and pollution research, 30, (2023), 95634-95647, Doi: <https://doi.org/10.1007/s11356-023-29024-4>
- Khaledi Maki L, Maleki A, Rezaee R. LED-activated immobilized Fe-Ce-N tri-doped TiO₂ nanocatalyst on a glass bed for photocatalytic degradation organic dye from aqueous solutions. Environmental Technology and Innovation, 15, (2019), 100411 - 100425, DOI: <https://doi.org/10.1016/j.eti.2019.100411>
- Akl Awwad, Novel approach for sulphur nanoparticles using Albizia Julibrissin fruits extract, Advanced materials letters, 6, (2015), 235-238, DOI: <https://doi.org/10.5185/amlett.2015.5792>
- Najmeh Ahmadpour, Mohammad Hossein Sayadi, Sara Sobhani, Mahmood Hajiani, Photocatalytic degradation of model pharmaceutical pollutant by novel magnetic TiO₂@ZnFe₂O₄/Pd nanocomposite with enhanced photocatalytic activity and stability under solar light irradiation, Journal of environmental management, 271, (2020), DOI: <https://doi.org/10.1016/j.jenvman.2020.110964>
- Ali T, Tripathi P, Ameer Azam, Waseem Raza, Arham S Ahmed et al. Photocatalytic performance of Fe-doped TiO₂ nanoparticles under visible-light irradiation. Mater. Res. Express, 4, (2017), 015022 - 015035. DOI: <https://doi.org/10.1088/2053-1591/aa576d>
- HamadianM, Reisi-VananiA, Behpour M, Esmaeily A S, Synthesis and characterization of Fe, S-codoped TiO₂ nanoparticles: Application in degradation of organic water pollutants, Desalination 281(2011) 319-324 <https://doi.org/10.1016/j.desal.2011.08.028>
- Muhammad Imran, Zohaib Saeed, Muhammad Pervaiz, Kashif Mehmood, Rabia Ejaz, Umer Younas, Hafiz Amir Nadeem, Shah Hussain, Enhanced visible light photocatalytic activity of TiO₂ co-doped with Fe, Co, and S for degradation of Congo red, Spectrochimica Acta Part A: Molecular and Biomolecular Spectroscopy, 255 (2021) 119644 <https://doi.org/10.1016/j.saa.2021.119644>
- Aida Doroudian, Mahdih Emadi, Reza Hosseinzadeh, Parvaneh Maghami, Biological and molecular effects of pesticides on human health, Pesticides, (2022), 1-14, DOI: <https://doi.org/10.5772/intechopen.104811>
- Hyeonhan Lim, Mohammad Yusuf, Sehwan Song, Sung Kyun Park and Kang Hyun park, Efficient photocatalytic degradation of dyes using photo deposited Ag nanoparticles on ZnO structures: simple morphological control of ZnO, Royal society of Chemistry, 15, (2021), 8709-8717, DOI: <https://doi.org/10.1039/D0RA10945B>
- Vasiljevic Z.Z, Dojcinovic M.P, Vujanecvic J.D, Jankovic - Castvan.I, Ognjanovic M, Tadic N.B, Stojadinovic. S, Brankovic. G.O. Nikolic. M.V, Photocatalytic degradation of methylene blue under natural sunlight using iron titanate nanoparticles prepared by a modified sol-gel method, Royal Society open Science, 7, (2020), 1-14, DOI: <https://doi.org/10.1098/rsos.200708>
- Abdessalam Bouddouch, Brahim Akhsassi, Elhassan Amaterz, Bahcine Bakiz, Aziz Taoufyq, Sylvie Villain, Frederic Guinneton, Abdelaziz El Aamrani, Jean-Raymond Gavarri and Ab deljalil Benlhachemi, Photodegradation under UV light irradiation of various types of systems of organic pollutants in the presence of a performant BiPO₄, Catalysts, 12, (2022), 1-19, DOI: <https://doi.org/10.3390/catal12070691>
- Felix Aisien, Andrew Nosakhare Amenaghawon, E .F Ekpenisi, Photocatalytic decolourisation of industrial waste water from a soft drink company, Journal of Engineering and Applied Sciences, 9, 2014, 11-16,
- T. Sauer, G. Cesconeto Neto, H. J. Jose, R.F.P.M Moreira,



- Kinetics of photocatalytic degradation of reactive dyes in a TiO₂ slurry reactor, *Journal of Photo chemistry and Photobiology A: Chemistry*, 149, 2002, 147-154, DOI: [https://doi.org/10.1016/S1010-6030\(02\)00015-1](https://doi.org/10.1016/S1010-6030(02)00015-1).
21. Y.M.Hunge, A.A Yadav, Seok- won kang, Hyunmin kim, Photocatalytic degradation of tetracycline antibiotics using hydrothermally synthesized two - dimensional molybdenum disulfide/titanium dioxide composites, *Journal of Colloid and Interface Science*, 606, 2022, 454-463, DOI: <https://doi.org/10.1016/j.jcis.2021.07.151>.
 22. Muhammad Adeel, Muhammad Saeed, Iltaf khan, Majid Muneer, and Nadia Akram Synthesis and characterization of Co- ZnO and Evaluation of its photocatalytic activity for photodegradation of methyl orange, *Acs Omega*, 6, (2021), 1426-1435, DOI: <https://doi.org/10.1021/acsomega.0c05092>.
 23. S. Sibmah and E.K. Kirupa Vasam, An efficient photocatalytic degradation of Quinalphos pesticide under visible light using zinc oxide / magnesium oxide nanocomposites as a novel photocatalyst, *Indian journal of chemistry*, 61, (2022), 901-908, DOI: <https://doi.org/10.56042/ijc.V61i8.59489>.
 24. Asmaa A. Abd-Allah, Yasser M.Z. Ahmed, Said M. El-Sheikh, Ahmed O. Youseef, Amira M.M. Amin, Synthesis of Zinc aluminate nanoparticles from aluminium /zinc sludge for degradation of brilliant cresyl blue under visible light, *Journal of water environment and nanotechnology*, 7, (2022), 288-305, DOI: <https://doi.org/10.22090/jwent.2022.03.005>.
 25. Ghader Hosseinzadeh, Innovative synthesis of TiO₂ nanorod/WO₃ nanoflakes hetero junction photocatalyst for visible light degradation of Nintenpyram insecticide, *Journal of water environment and nanotechnology*, 7, (2022), 230-240, DOI: <https://doi.org/10.22090/jwent.2022.03.001>.